การเปลี่ยนสัญญาณแสงแบบโซลิตรอนแสงมืดและแสงสว่างโดยใช้หลักการของโพรงสั่นพ้องระดับนาโนเมตรด้วยระบบกรองสัญญาณแสงแอ็ด/ดร็อป

Dark-Bright Soliton Conversion Control Using Double Nanoring Resonators within an Add/Drop Filter

ปรีชา ยุพาพิน[1], **สุขุม จุฬาจัตตุรศิระรัตน์**[2]

Received: September, 2013; Accepted: June, 2014

บทคัดย่อ

วัตถุประสงค์ในการออกแบบระบบการเปลี่ยนโซลิตรอนแสงมืด และสว่างโดยสามารถควบคุม และออกแบบขนาดของแสงโดยอุปกรณ์กรองแสง แอ็ด/ดร็อป เมื่อมีการควบคุมโดยแสงมืด และโซลิตรอนแสงสว่าง ในบทความนี้ อธิบายถึงพฤติกรรมของแสงมืดและแสงสว่างในการวิเคราะห์เกี่ยวพันเชิงแสงในการประยุกต์สามารถ นำเอาแสงที่ถูกกักไว้ในหลุมศักคิ์นำมาใช้ใหม่อีกครั้ง คืมคีปแสง และสามารถสร้างคืมคีบแสงแบบหลายช่องสัญญาณ

คำสำคัญ : ปฏิกิริยารีดักชันชนิดเร่งด้วยแสง; โครเมียมวาเลนท์ซีหก; ซิลเวอร์โด๊ปซิงค์ออกไซด์; จลนพลศาสตร์

[1] *คณะวิทยาศาสตร์ สถาบันเทคโนโลยีพระจอมเกล้าเจ้าคุณทหารลาดกระบัง*

[2] *คณะอุตสาหกรรมและเทคโนโลยี มหาวิทยาลัยเทคโนยีราชมงคลอีสาน วิทยาเขตขอนแก่น*

E - mail : kypreech@kmitl.ac.th, terrybrogards@hotmail.com

Abstract

We propose a novel system of a dark-bright soliton pulse conversion that can be dynamically controlled by the desired input signal within an add/drop optical filter, where the dark solition signals are controlled, tuned and amplified by the input bright soliton. In this paper, the dynamic behavior of dark-bright soliton interaction is analyzed and described. The optical storages are embedded within the add/drop optical filter system, whereas the generated optical signals can be stored and amplified. In application, the storage signals can be configured to be an optical trapping tool/potential well which is known as optical tweezers, where the high field peak signal or well can be formed the trapping tool.

Keywords : Dynamic dark-bright soliton conversion; Dynamic wells

Introduction

Dark-bright soliton control within the add/drop filter has been investigated clearly by the authors in reference (K. Sarapat et al., 2009), where one of the advantages is that the dark soliton peak signal is always low level, which can be useful for secured signal communication in the transmission link. The other application is formed when the high optical field is configured as an optical tweezer or potential well, which is available for use as an atom/molecule trapping tool. Optical tweezers technique has become a powerful tool for manipulation of micrometer-sized particles in three spatial dimensions (A. Ashkin et al., 1986; P. Minzioni et al., 2008). Initially, the useful static tweezer is recognized, and the dynamic tweezer is now realized in the practical work. Typically by using the continuous-wave (cw) lasers, the spatial control of atoms, beyond their trapping in stationary potentials, has been continuously gaining importance in investigations of ultra cold gases and in the application of atomic ensembles and single atoms for cavity quantum electrodynamics (QED) and quantum information studies. The recent progress includes the trapping and control of single atoms in dynamic potentials (S. Bergamini et al., 2004; D. D. Yavuz et al., 2006), the sub-micron positioning of individual atoms with standing-wave potentials (D. Schrader et al., 2004; J. A. Sauer et al., 2004), micro-structured and dynamic traps for Bose-Einstein condensates (T. P. Meyrath et al., 2005; V. Boyer et al., 2006; A.V. Carpentier et al., 2008).

THEORY BACKGROUND

In this investigation, we are looking for a stationary dark soliton pulse, which is introduced into the multistage micro-ring resonators as shown in references (K. Sarapat et al., 2009; S. Mitatha et al., 2009; P.P. Yupapin and N. Pornsuwan-charoen. 2009). The input optical field (Ei1) of the dark soliton pulse and the optical field (Ei2) of the bright soliton pulse (pump signal) at add port are given by

$$E_{i1}(t) = A\tanh\left[\frac{T}{T_0}\right]\exp\left[\left(\frac{z}{2L_D}\right)-i\omega_0 t\right], \qquad (1a)$$

$$E_{i2}(t) = A\,\mathrm{sech}\left[\frac{T}{T_0}\right]\exp\left[\left(\frac{z}{2L_D}\right)-i\omega_0 t\right], \qquad (1b)$$

where A and z are the optical field amplitude and propagation distance, respectively. T is a soliton pulse propagation time in a frame moving at the group velocity, $T=t-\beta_1 * z$,where β_1 and β_2 are the coefficients of the linear and second-order terms of Taylor expansion of the propagation constant. $L_D = T_0^2/|\beta_2|$ is the dispersion length of the soliton pulse. T_0 in equation is a soliton pulse propagation time at initial input (or soliton pulse width), where t is the soliton phase shift time, and the frequency shift of the soliton is ω_0 This solution describes a pulse that keeps its temporal width invariance as it propagates, and thus is called a temporal soliton. When a soliton peak intensity $\left(\left|\beta_2/\Gamma T_0^2\right|\right)$ is given, then T_0 is known. For the soliton pulse in the microring device, a balance should be achieved between the dispersion length (L_D) and the nonlinear length ($L_{NL}=1/\Gamma\phi_{NL}$), where $\Gamma=n_2*k_0$, is the length scale over which dispersive or nonlinear effects makes the beam become wider or narrower. For a soliton pulse, there is a balance between dispersion and nonlinear lengths, hence $L_D = L_{NL}$.

When light propagates within the nonlinear material (medium), the refractive index (n) of light within the medium is given by

$$n = n_0 + n_2 I = n_0 + \frac{n_2}{A_{eff}}P, \qquad (2)$$

where n_0 and n_2 are the linear and nonlinear refractive indexes, respectively. I and P are the optical intensity and optical power, respectively. The effective mode core area of the device is given by Aeff. The resonant output is formed,

thus, the normalized output of the light field is the ratio between the output and input fields [E_{out}(t) and $E_{in}(t)$] in each roundtrip, which is given by

$$\left|\frac{E_{out}(t)}{E_{in}(t)}\right|^2 = (1-\gamma)\left[1-\frac{(1-(1-\gamma)x^2)\kappa}{(1-x\sqrt{1-\gamma}\sqrt{1-\kappa})^2+4x\sqrt{1-\gamma}\sqrt{1-\kappa}\sin^2(\frac{\phi}{2})}\right] \quad (3)$$

The close form of Eq. (3) indicates that a ring resonator in this particular case is very similar to a Fabry–Perot cavity, which has an input and output mirror with a field reflectivity, $(1-\kappa)$, and a fully reflecting mirror. κ is the coupling coefficient, and $x=exp(-\alpha L/2)$represents a roundtrip loss coefficient, $\phi_0=kLn_0$ and $\phi_{NL}=kLn_2|E_{in}|^2$ are the linear and nonlinear phase shifts, $k=2\pi/\lambda$ is the wave propagation number in a vacuum, where L and α are waveguide length and linear absorption coefficient, respectively. γ is fractional coupler in tensity loss.

In this work, the iterative method is introduced to obtain the results as shown in Eq. (3), and similarly, when the output field is connected and input into the other ring resonators.

To retrieve the signals from the chaotic noise, we propose to use the add/drop device with the appropriate parameters. This is given in the following details. The optical circuits of ring-resonator add/drop filters for the through and drop port can be given by Eqs. (4) and (5), respectively (K. Sarapat et al., 2009; A.V. Carpentier et al., 2008)

$$\left|\frac{E_{t1}}{E_{in}}\right|^2 = \frac{(1-\kappa_1)-2\sqrt{1-\kappa_1}\cdot\sqrt{1-\kappa_2}e^{-\frac{\alpha}{2}L}\cos(k_nL)+(1-\kappa_2)e^{-\alpha L}}{1+(1-\kappa_1)(1-\kappa_2)e^{-\alpha L}-2\sqrt{1-\kappa_1}\cdot\sqrt{1-\kappa_2}e^{-\frac{\alpha}{2}L}\cos(k_nL)} \quad (4)$$

$$\left|\frac{E_{t2}}{E_{in}}\right|^2 = \frac{\kappa_1\kappa_2 e^{-\frac{\alpha}{2}L}}{1+(1-\kappa_1)(1-\kappa_2)e^{-\alpha L}-2\sqrt{1-\kappa_1}\cdot\sqrt{1-\kappa_2}e^{-\frac{\alpha}{2}L}\cos(k_nL)} \quad (5)$$

where E_{t1} and E_{t2} represent the optical fields of the through and drop ports, respectively. $\beta = kn_{\text{eff}}$ is the propagation constant, n_{eff} is the effective refractive index of the waveguide, and the circumference of the ring is $L=2\pi R$, with R as the radius of the ring. In the following, new parameters will be used for simplification with $\phi = \beta L$ as the phase constant. The chaotic noise cancellation can be managed by using the specific parameters of the add/drop device, and the required signals can be retrieved by the specific users. $\kappa_1$and κ_2 are the coupling coefficient of the add/drop filters, $k_n=2\pi/\lambda$ is the wave propagation number for in a vacuum, and

where the waveguide (ring resonator) loss is α = 0.5 dBmm^{-1}. The fractional coupler intensity loss is γ = 0.1. In the case of the add/drop device, the nonlinear refractive index is neglected.

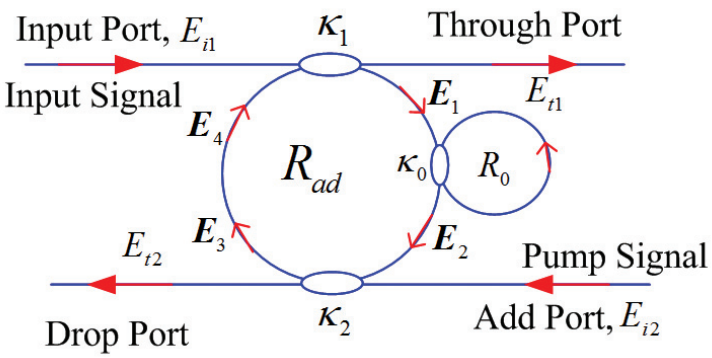

Figure 1 A schematic diagram of storage optical tweezers, where a single nanoring resonator

The schematic diagram of the optical tweezers storage is designed and shown in Figure 1. In operation, to form the storage unit, a nanoring resonator is embedded within the add/drop optical filter in the system. The nanoring resonator radius (R_0) and the coupling coefficient (κ) are 100nm and 0.15, respectively. In order to make the system associate with the practical device (L.J. Heyderman et al., 2004), in the system design, the dark soliton pulse is input into the input port through the coupler with the coupling coefficient is κ_1 = 0.35. It is partially input into the nanoring resonator with 20,000 roundtrips, where the storage signal is observed, the memory time is noted.

Single Nanoring Resonator

From Figure 1, when a light propagates through the first coupler with the coupling coefficient κ_1, where the optical outputs are given by Eqs. (6) and (7).

$$E_{t1} = \sqrt{1-\gamma_1}\left[j\sqrt{\kappa_1}E_4 + \sqrt{1-\kappa_1}E_{i1} \right] \quad (6)$$

$$E_1 = \sqrt{1-\gamma_1}\left[j\sqrt{\kappa_1}E_{i1} + \sqrt{1-\kappa_1}E_4 \right] \quad (7)$$

One of the optical fields passes through the coupler of a nanoring resonator with the coupling coefficient κ_0 as shown in Figure 2. The optical outputs are given by Eqs. (8), (9) and (10).

$$E_2 = \sqrt{1-\gamma_0}\left[j\sqrt{\kappa_0}E_{r2} + \sqrt{1-\kappa_0}E_1 \right] \tag{8}$$

$$E_{r1} = \sqrt{1-\gamma_0}\left[j\sqrt{\kappa_0}E_1 + \sqrt{1-\kappa_0}E_{r2} \right] \tag{9}$$

$$E_{r2} = E_{r1}e^{-\frac{\alpha}{2}L_0 - jk_nL_0} \tag{10}$$

where the circumference of a nanoring is L_0 ($L = 2\pi R_0$; the radius is R_0), the coupling coefficient is κ_0. The intensity attenuation coefficient of the nanoring is α, and the wave propagation constant is k_n.

$$E_2 = \sqrt{(1-\gamma_0)(1-\kappa_0)}E_1 - \frac{(1-\gamma_0)\kappa_0 E_1 e^{-\frac{\alpha}{2}L_0 - jk_nL_0}}{1-\sqrt{(1-\gamma_0)(1-\kappa_0)}e^{-\frac{\alpha}{2}L_0 - jk_nL_0}} \tag{11}$$

When the output light from Eq. (11) propagates through the second coupler of the add/drop optical filter with the coupling coefficient κ_2. The optical outputs are given by Eqs. (12), (13) and (14).

$$E_{t2} = \sqrt{1-\gamma_2}\left[\sqrt{1-\kappa_2}E_{i2} + \sqrt{\kappa_2}E_2 \right] \tag{12}$$

$$E_3 = \sqrt{1-\gamma_2}\left[\sqrt{1-\kappa_2}E_2 + j\sqrt{\kappa_2}E_{i2} \right] \tag{13}$$

$$E_4 = E_3 e^{-\frac{\alpha}{2}\frac{L_{ad}}{2} - jk_n\frac{L_{ad}}{2}} \tag{14}$$

where the circumference of an optical add/drop filter is L_{ad} ($L_{ad} = 2\pi R_{ad}$; the radius is R_{ad}), the first and second coupling coefficient of the add/drop are κ_1 and κ_2, respectively.

Substitute E_2 from Eq. (11) into Eq. (13) and E_3 from Eq. (13) into (14), yield

$$E_4 = j\sqrt{(1-\gamma_2)(1-\kappa_2)}E_{i2}e^{-\frac{\alpha}{2}\frac{L_{ad}}{2} - jk_n\frac{L_{ad}}{2}} + \sqrt{(1-\gamma_2)(1-\kappa_2)}E_2E_1\left(e^{-\frac{\alpha}{2}\frac{L_{ad}}{2} - jk_n\frac{L_{ad}}{2}} \right)^2 \tag{15}$$

From Eq. (7), the field E1 is expressed by

$$E_1 = \frac{j\sqrt{(1-\gamma_1)\kappa_1}E_{i1} + jKE_{i2}e^{-\frac{\alpha}{2}\frac{L_{ad}}{2} - jk_n\frac{L_{ad}}{2}}}{1 - KE_2\left(e^{-\frac{\alpha}{2}\frac{L_{ad}}{2} - jk_n\frac{L_{ad}}{2}}\right)^2} \tag{16}$$

where $K = \sqrt{(1-\gamma_1)(1-\gamma_2)(1-\kappa_1)(1-\kappa_2)}$

The through port output field (E_{t1}) is given by

$$\begin{aligned} E_{t1} = & -\sqrt{(1-\gamma_1)(1-\gamma_2)(\kappa_1)(1-\kappa_2)}e^{-\frac{\alpha}{2}\frac{L_{ad}}{2} - jk_n\frac{L_{ad}}{2}} \\ & + j\sqrt{(1-\gamma_1)(1-\gamma_2)(\kappa_1)(\kappa_2)}E_2\left(e^{-\frac{\alpha}{2}\frac{L_{ad}}{2} - jk_n\frac{L_{ad}}{2}}\right)^2 \\ & \times\sqrt{1-\gamma_1}\left\{\frac{j\sqrt{\kappa_1}E_{i1} + j\sqrt{(1-\gamma_2)(\kappa_1)(\kappa_2)}E_{i2}e^{-\frac{\alpha}{2}\frac{L_{ad}}{2} - jk_n\frac{L_{ad}}{2}}}{1-\sqrt{(1-\gamma_1)(1-\gamma_2)(1-\kappa_1)(1-\kappa_2)}E_2\left(e^{-\frac{\alpha}{2}\frac{L_{ad}}{2} - jk_n\frac{L_{ad}}{2}}\right)^2}\right\} \end{aligned} \tag{17}$$

The through port output power (P_{t1}) is given by

$$P_{t1} = \left|E_{t1}\right|^2. \tag{18}$$

The drop port output field (E_{t2}) is given by

$$\begin{aligned} E_{t2} = & \sqrt{(1-\gamma_2)(1-\kappa_2)}E_{i2} + j\sqrt{(1-\gamma_2)(\kappa_2)}E_2e^{-\frac{\alpha}{2}\frac{L_{ad}}{2} - jk_n\frac{L_{ad}}{2}} \\ & \times j\sqrt{1-\gamma_1}\left[\frac{\sqrt{\kappa_1}E_{i1} + \sqrt{(1-\gamma_2)(1-\kappa_1)(1-\kappa_2)}e^{-\frac{\alpha}{2}\frac{L_{ad}}{2} - jk_n\frac{L_{ad}}{2}}}{1-\sqrt{(1-\gamma_1)(1-\gamma_2)(1-\kappa_1)(1-\kappa_2)}E_2\left(e^{-\frac{\alpha}{2}\frac{L_{ad}}{2} - jk_n\frac{L_{ad}}{2}}\right)^2}\right] \end{aligned} \tag{19}$$

The drop port output power (P_{t2}) is

$$P_{t2} = \left|E_{t2}\right|^2. \tag{20}$$

Double Nanoring Resonator

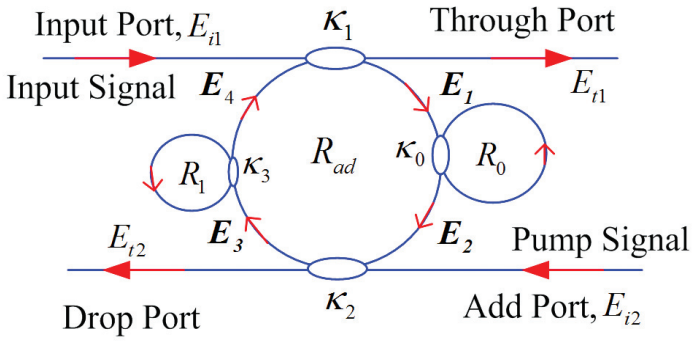

Figure 3 A schematic diagram of storage optical tweezers, where a double nanoring resonators

The schematic diagram of the double nanoring resonator is as shown in Figure 3 Similarity, the through port output field (E_{t1}) is expressed by

$$E_{t1} = AE_{i1} - BE_{i2}e^{\frac{\alpha L}{2}-jk_n\frac{L}{2}} - \left[\frac{CE_{i1}\left(e^{\frac{\alpha L}{2}-jk_n\frac{L}{2}}\right)^2 + DE_{i2}\left(e^{\frac{\alpha L}{2}-jk_n\frac{L}{2}}\right)^3}{1-E\left(e^{\frac{\alpha L}{2}-jk_n\frac{L}{2}}\right)^2}\right], \quad (21)$$

When $A = \sqrt{(1-\gamma_1)(1-\gamma_2)}$,

$B = \sqrt{(1-\gamma_1)(1-\gamma_2)\kappa_1(1-\kappa_2)}E_{0L}$,

$C = \kappa_1(1-\gamma_1)\sqrt{(1-\gamma_2)\kappa_2}E_2E_{0L}$,

$D = (1-\gamma_1)(1-\gamma_2)\sqrt{\kappa_1(1-\kappa_1)\kappa_2(1-\kappa_2)}E_2E_{0L}^2$ and

$E = \sqrt{(1-\gamma_1)(1-\gamma_2)(1-\kappa_1)(1-\kappa_2)}E_2E_{0L}$

$$E_{0L} = \sqrt{(1-\gamma_3)(1-\kappa_3)}E_3 - \frac{(1-\gamma_3)(\kappa_3)E_3e^{-\frac{\alpha}{2}L_3-jk_nL_3}}{1-\sqrt{(1-\gamma_3)(1-\kappa_3)}e^{-\frac{\alpha}{2}L_3-jk_nL_3}}$$

The through port output power (P_{t1}) is

$$P_{t1} = |E_{t1}|^2. \quad (22)$$

The drop port output field (E_{t2}) is given by

$$E_{t2} = aE_{i2} - \left[\frac{bE_{i1} e^{-\frac{\alpha L}{2} - jk_n \frac{L}{2}} + cE_{i2} \left(e^{-\frac{\alpha L}{2} - jk_n \frac{L}{2}} \right)^2}{1 - E \left(e^{-\frac{\alpha L}{2} - jk_n \frac{L}{2}} \right)^2} \right], \qquad (23)$$

when $a = \sqrt{(1-\gamma_2)(1-\kappa_2)}$,

$b = \sqrt{\kappa_1(1-\gamma_1)\kappa_2(1-\gamma_2)}E_2$, and

$c = (1-\gamma_2)\sqrt{(1-\gamma_1)(1-\kappa_1)\kappa_2(1-\kappa_2)}E_2E_{0L}$.

The drop port output power (P_{t2}) is

$$P_{t2} = \left|E_{t2}\right|^2. \qquad (24)$$

RESULT AND DISCUSSION

The suitable radii of a nanoring resonator parameter is used, such as $R_0 = 100nm$, $R_{ad} = 15\mu m$ and $R_2 = 50nm$. In order to make the system associate with the practical device (L.J. Heyderman et al., 2004), the selected parameters of the system are fixed to $\lambda_0 = 1.55\mu m$, $n_0 = 3.34$, $n_2 = 2.2\times10^{-13}\ m^2/W$ (InGaAsP/InP waveguide). The effective core area is $A_{eff} = 0.10\ \mu m^2$ for a nanoring resonator. The waveguide and coupling loses are a $\alpha = 0.5 \text{dBmm}^{-1}$ and $\gamma = 0.1$, respectively, and the simulated results are generated at wavelength center, $\lambda_0 = 1.4\mu m$ and $1.5\mu m$.

The optical storage signals within the add/drop system is as shown in Figure 4 We found that the storage time is *1.2 ns*, the trapping signal (tool) width of the storage signal in add/drop at the through and drop ports are *19.2*, *17.6* and *18.6* nm, respectively. In Figures 4(a) – 4(b), the trapping tools in the form of potential wells are seen, which can be used for atom/molecule trapping tools. The potential well dept (peak valley) can be controlled by adjusting the system parameters, for instance, the bright soliton input power at the add port and the coupling coefficients. The potential well of the trapping tool is tuned to be the single well and seen at the add port, as shown in Figure 4(c). In application, the optical trapping tools in the design system can be tuned and amplified as shown in Figure 4 Therefore, the tunable optical trapping tool can be controlled by the dark-bright soliton collision within the add/drop optical system by

adjusting the parameters of the input power at the input and add ports, respectively. The output power at the through port is shown in Figure 4(c), where the single potential well with the optical power of 15 W is seen, which is ready to use in the required application.

More result is as shown in Figure 5, where in Figure 5 shows the result of the optical trapping storage signals in the add/drop system, where the coupling coefficients are $\kappa_0 = 0.7$, $\kappa_1 = 0.35$, $\kappa_2 = 0.1$ and $\kappa_3 = 0.9$, respectively. To realize the tunability of the device by tuning or controlling the pump signal at add port as shown in Figure 1. The ring radii are $R_{add} = 15\mu m$, $R_0 = 10\mu m$ and $R_1 = 6\mu m$.. The A_{eff} are 0.5, 0.25 and $0.05\mu m^2$ for add/drop, right and left ring resonators, respectively, where the storage trapping tool (output signal), through port and drop port signals are seen. In application, the term dynamics can be realized and available for dynamic wells/trapping tools control, which means the movement of trapping tool/wells can be formed within the system.

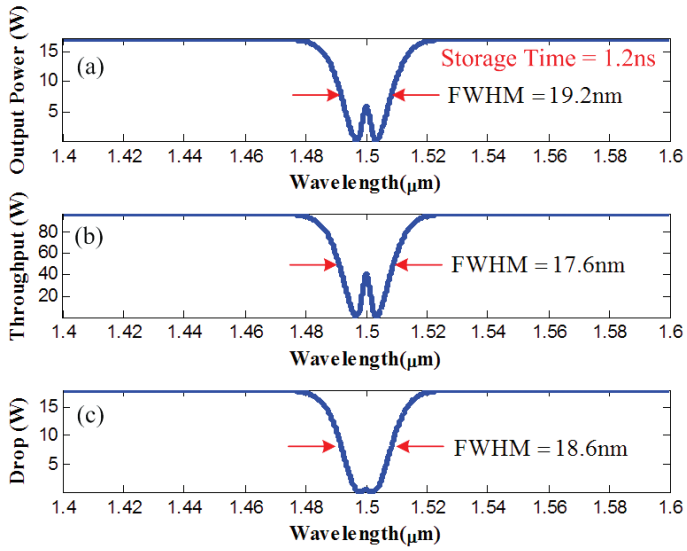

Figure 4 Simulation result of the optical trapping (storage) signals in the add/drop system, where $R_{ad} = 15\mu m$ and $R_{ring} = 100nm$, $\kappa = 0.15$, $\kappa_1 = 0.35$ and $\kappa_2 = 0.1$. (a) storage trapping, (b) through port signal, and (c) drop port signal.

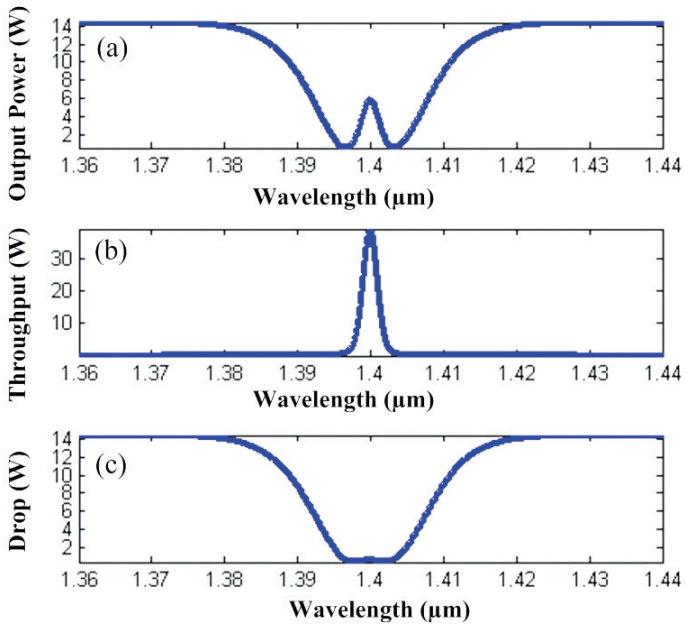

Figure 5 Simulation results, where (a) the optical tweezers storage signals (dark-bright collision) in the add/drop system, where the storage signal (output signal), (b) bright conversion at through port signal, and (c) dark conversion at drop port signal are seen.

More result is as shown in Figure 6, where in Figure 6 shows the result of the optical trapping storage signals in the add/drop system, where the coupling coefficients are $\kappa_0 = 0.7$, $\kappa_1 = 0.35$, $\kappa_2 = 0.1$ and $\kappa_3 = 0.5$, respectively. To realize the tunability of the device by tuning or controlling the pump signal at add port as shown in Figure 1. The nanoring radii are used the same as the previous simulated results, where the optical trapping storage signals (output signal) are shown in Figure 6. The optical trapping and storage signals in the add/drop system are (a) bright conversion, (b) output signal through right nanoring resonator radius R_0, (c) dark-bright collision, (d) output signal through left nanoring resonator radius R_1, (e) output at through port and (f) dark conversion at drop port.

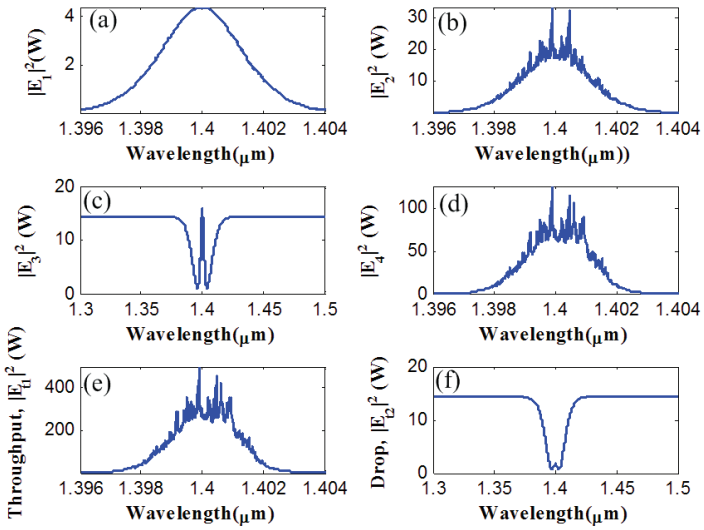

Figure 6 Simulation results of the optical trapping and storage signals in the add/drop system, where (a) bright conversion, (b) output signal through right nanoring resonator radius R_0, (c) dark-bright collision, (d) output signal through left nanoring resonator radius R_1, (e) output at through port and (f) dark conversion at drop port.

CONCLUSION

We have analyzed and shown that the dynamic optical trapping tools can be generated by using dark and bright solitons collision control within the add/drop filter. The trapping tool storage can be performed by adding a nanoring resonator within design system, incorporating the add/drop multiplexer. By using the reasonable dark-bright soliton input power, the dynamic optical trapping signal can be controlled and stored within the add/drop filter. Hence, the dynamic behavior can be controlled and used in the dynamic application. The smallest trapping tool width (full width at half maximum, FWHM) of 11 nm is obtained. The maximum power and memory time of 50 W and 1.2 ns are obtained respectively. In application, such a behavior can be used to confine the suitable size of light pulse or molecule, which can be employed in the same way of the optical trapping tools (tweezers). But in this case the terms dynamic probing is become the realistic function, where the trapped pulse or molecule within the period of time (memory) is plausible. Moreover, the multiple trapping

tools/wells storage configuration is allowed the storage array of tweezers/wells, which is available for high density tweezers/wells storage and high capacity molecular transportation which will be our continuous work. The advantages of proposed system are the dynamic well can be stored and the array of wells can be generated for multiple tweezers/wells applications.

Acknowledgment

We would like to give the acknowledgment to King Mongkut's Institute of Technology Ladkrabang (KMITL), Bangkok 10520, Thailand for the language improvement and laboratory facilities.

References

K. Sarapat, N. Sangwara, K. Srinuanjan, P.P. Yupapin and N. Pornsuwancharoen. (2009). Novel dark-bright optical solitons conversion system and power amplification. **Opt. Eng.** 48:045004-7.

A. Ashkin, J.M. Dziedzic, J.E. Bjorkholm and S. Chu. (1986). Observation of a single-beam gradient force optical trap for dielectric particles. **Opt. Lett.** 11:288-290.

P. Minzioni, F. Bragheri, C. Liberale, E. D. Fabrizio, and I. Cristiani. (2008). A novel approach to fiber-optic tweezers: numerical analysis of the trapping efficiency. **IEEE J. Sel. Topics. in Quantum. Electron.** 14:151-157.

S. Bergamini, B. Darqui, M. Jones, L. Jacubowiez, A. Browaeys and P. Grangier. (2004). Holographic generation of microtrap arrays for single atoms by use of a programmable phase modulator. **J. Opt. Soc. Am. B.** 21:1889-1894.

D. D. Yavuz, P. B. Kulatunga, E. Urban, T. A. Johnson, N. Proite, T. Henage, T. G. Walker and M. Saffman. (2006). Fast ground state manipulation of neutral atoms in microscopic optical traps. **Phys. Rev. Lett.** 96:063001.

D. Schrader, I. Dotsenko, M. Khudaverdyan, Y. Miroshnychenko, A. Rauschenbeutel and D. Meschede. (2004). Neutral atom quantum register. **Phys. Rev. Lett.** 93:150501.

J. A. Sauer, K. M. Fortier, M. S. Chang, C. D. Hamley and M. S. Chapman. (2004). Submicrometer position control of single trapped neutral atoms. **Phys. Rev. A.** 69:051804(R).

T. P. Meyrath, F. Schreck, J. L. Hanssen, C.-S. Chuu and M. G. Raizen. (2005). Bose-Einstein condensate in a box. **Phys. Rev.** A, 71:041604(R).

V. Boyer, R. M. Godun, G. Smirne, D. Cassettari, C. M.Chandrashekar, A. B. Deb, Z. J. Laczik and C. J. Foot. (2006). Dynamic manipulation of Bose-Einstein condensates with a spatial light modulator. **Phys. Rev.** A, 73:031402(R).

A.V. Carpentier, J. Belmonte-Beitia, H. Michinel and V.M. Perez-Garcia. (2008). Laser tweezers for atomic solitons. **J. of Mod. Opt.** 55:2819-2829.

V. Milner, J. L. Hanssen, W. C. Campbell and M. G.Raizen. (2001). Optical billiards for atoms. **Phys. Rev. Lett.** 86:1514-1516.

S. Mitatha, N. Pornsuwancharoen and P.P.Yupapin. (2009). A simultaneous short-wave and millimeter-wave generation using a soliton pulse within a nano-waveguide. **IEEE Photon. Technol. Lett.** 21:932-934.

P.P. Yupapin and N. Pornsuwancharoen. (2009). Proposed Nonlinear Microring Resonator Arrangement for Stopping and Storing Light. **IEEE Photon. Technol. Lett.** 21:404-406.

L.J. Heyderman, M. Kläui, B. Nöhammer, C.A.F. Vaz, J.A.C. Bland,and C. David. (2004). Fabrication of nanoscale magnetic ring structures and devices. **Microelectronic Engineering.** 73-74:780-784.